DOI: 10.1002/ejoc.201000335

A Joint Experimental and Theoretical Investigation on Nonlinear Optical (NLO) Properties of a New Class of Push–Pull Spirobifluorene Compounds

Fabio Rizzo,[a,b] Marco Cavazzini,[a,b] Stefania Righetto,[c] Filippo De Angelis,[d] Simona Fantacci,[d] and Silvio Quici*[a,b]

Keywords: Spiro compounds / Nonlinear optics / Ab initio calculations / Push–pull molecules

A new class of push–pull spirobifluorene compounds **1**–**5** has been synthesized. The nonlinear optical (NLO) properties (first and second hyperpolarizability β and γ, respectively) of spirobifluorene derivatives have been investigated for the first time using electric field induced second harmonic (EFISH) and third harmonic generation (THG) methods. Moreover, a comparison with the corresponding push–pull fluorene monomers **1a**–**5a** was carried out. Besides the experimental data, ab initio theoretical calculations on structural, electronic, and optical properties were carried out for all compounds. The analyses indicate that an increase in the β and γ values occur on passing from monomers to dimers without compromising the optical transparency.

Introduction

In recent years the design and synthesis of organic compounds that exhibit nonlinear optical (NLO) properties has received particular attention because of their possible applications in various fields, including telecommunications and optical data storage and processing.[1] Much effort have been aimed at identifying relationships between organic structure and nonlinear optical activities so that these systems can be made more efficient.[2–6] In particular, since the nonlinear optical properties of a compound stems from a nonlinear polarization induced by a beam of high intensity (typically a laser), it was soon clear that the ability of a compound to show second order NLO phenomena should be related to the degree of charge separation in the ground state. Until now, most of the organic molecules characterized by second order NLO properties contain electron-donating (D) and electron-withdrawing (A) groups linked through a conjugated π-spacer ("push–pull" systems). According to the Oudar two-states model,[7] it is well-established that the first order hyperpolarizability β of push–pull chromophores with D-π-A linear structure increases upon increasing either the length of the π-conjugated system or the strength of both donor and acceptor groups.

The organization of push–pull chromophores in structurally oriented molecular architectures can be another interesting factor that can be used to amplify the non linear optical properties.

In molecular multichromophoric systems, the overall hyperpolarizability β arises from the contributions of the β value of each of the chromophoric units along the molecular dipole axis, whereas in the case of bulk materials, the NLO susceptibility is related to the β value of the chromophores and on their degree of orientation in the multilayer. In this sense, data has been reported in the literature concerning multichromophoric molecular systems such as calixarenes[8–10] and cyclotetrasiloxane rings,[11] or multilayered organized systems, where NLO molecules have be assembled by using zirconium phosphate–phosphonate ($ZrPO_x$) techniques,[12–14] layer-by-layer siloxane-based self-assembly,[15] or Langmuir–Blodgett techniques.[16]

An interesting way to prepare geometrically oriented push–pull bichromophoric systems is to covalently arrange them into a highly delocalized structure with an orthogonal spatial arrangement, as in the case of 9,9′-spirobifluorene, where two fluorenes are connected through an sp^3-hybridized carbon atom (Figure 1).

Indeed, the chemical versatility of spirobifluorene allows the introduction of different chemical functional groups in the 2,2′ and 7,7′ positions, thus affording symmetric or asymmetric compounds.[17] Therefore, when electron-donating and electron-accepting groups are introduced in these positions, the resulting molecule formerly consists of two push–pull halves with a mutually perpendicular arrangement with a non-vanishing resulting dipole moment.[18] So

[a] Istituto di Scienze e Tecnologie Molecolari (ISTM), Consiglio Nazionale delle Ricerche,
via C. Golgi 19, 20133 Milano, Italy
[b] Polo Scientifico e Tecnologico (PTS), Consiglio Nazionale delle Ricerche (CNR),
via Fantoli 16/15, 20138 Milano, Italy
Fax: +39-02-50314159
E-mail: silvio.quici@istm.cnr.it
[c] Dipartimento CIMA "Lamberto Malatesta", Università degli Studi di Milano and UdR dell'INSTM,
via Venezian 21, 20133, Milano, Italy
[d] Istituto di Scienze e Tecnologie Molecolari (ISTM),
c/o Dipartimento di Chimica, Università degli Studi di Perugia,
Consiglio Nazionale delle Ricerche,
via Elce di Sotto 8, 06123 Perugia, Italy

 WILEY InterScience DISCOVER SOMETHING GREAT © 2010 Wiley-VCH Verlag GmbH & Co. KGaA, Weinheim

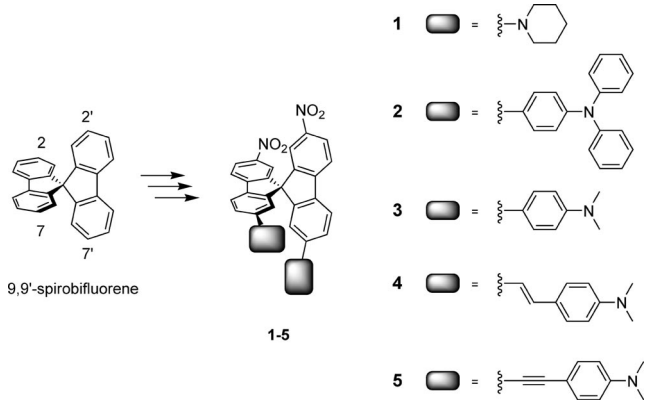

Figure 1. Schematic representation of 9,9′-spirobifluorene and synthesized push–pull derivatives **1**–**5**.

this molecule represents an unconventional push–pull system that, in principle, can show interesting second order nonlinear optical properties.

Although several spirobifluorene compounds bearing donor and acceptor residues have been synthesized and employed for example as dyes[19–21] or as ambipolar transporting molecules,[22,23] to the best of our knowledge, no experimental data on their hyperpolarizability β have yet been reported. The first hyperpolarizability of spiro-linked push–pull polyenes, where several 1,4-cyclohexadiene rings are connected by the tetrahedral sp^3 carbon atoms and electron-donating and electron-withdrawing groups are introduced in the terminal 1,4-cyclohexadiene rings, has been investigated by using ab initio and INDO/S molecular orbital calculations.[24] By comparing the obtained results for the spiro-linked polyenes with those calculated for the corresponding linear polyenes, it was concluded that these compounds behave as excellent second-order nonlinear optical materials from the standpoint of transparency and relatively large β values.[25] The second hyperpolarizability γ of 2,2′-diamino-7,7′-dinitro-9,9′-spirobifluorene has been experimentally measured through a Degenerate Four Wave Mixing (DFWM) procedure.[26] The value obtained was ten times that of the corresponding 2-amino-7-nitrofluorene monomer. Theoretical calculations reported for this same compound showed that intermolecular vibrational modes significantly contribute to the gas-phase second hyperpolarizability, although not to an extent that can explain the experimentally observed increase in the value of the dimer with respect to the monomer.[27,28]

In this paper we report the synthesis of five new spirobifluorene push–pull derivatives **1**–**5**, bearing a disubstituted amine and a nitro group in the 2,2′- and 7,7′-positions, respectively (Figure 1), in which electronic connection is guaranteed by a range of π-bridges. In order to gain a better insight into the linear and nonlinear optical properties of these bichromophoric systems, and to compare the related push–pull fluorene monomers **1a**–**5a**, a joint spectroscopic, experimental and theoretical approach was undertaken. The results are presented here.

Results and Discussion

Synthesis of Spirobifluorenes 1–5 and Related Fluorenes 1a–5a

The push–pull spirobifluorene compounds **1**–**5** were designed to gain information on the effect of conjugation and on the relationship between the donor moieties and the NLO properties. A disubstituted amino group (dialkyl or diaryl) and a nitro group were chosen as electron-donating and electron-withdrawing substituents, respectively. Furthermore, we decided to introduce a structural modification by varying the degree of unsaturation in the π-spacers that connect the amino group to the spirobifluorene unit. The synthetic strategy for the preparation of compounds **1**–**5** involved the synthesis of the key intermediate 2,2′-dibromo-7,7′-dinitro-9,9′-spirobifluorene (**8**), as reported in Scheme 1.

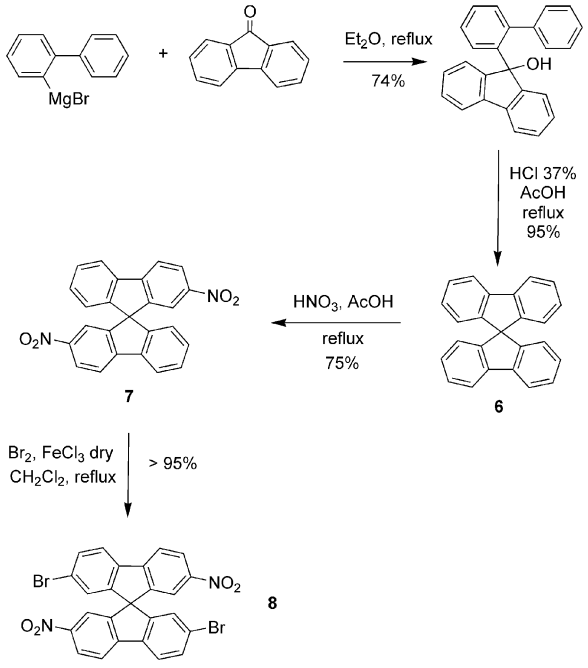

Scheme 1. Synthesis of 2,2′-dibromo-7,7′-dinitro-9,9′-spirobifluorene (**8**).

9,9′-Spirobifluorene (**6**) was prepared starting from commercially available 2-bromobiphenyl.[29] The reaction of the Grignard derivative of 2-bromobiphenyl with 9-fluorenone was followed by a condensation under acidic conditions to give **6** in 70% overall yield. Although the direct bromination of 9,9′-spirobifluorene is described in literature,[29] we had difficulty isolating pure 2,2′-dibromo-9,9′-spirobifluorene as also reported by other groups.[30] On the other hand, following the procedure described by Sutcliffe et al.,[31] **6** was easily subjected to double electrophilic aromatic substitution to afford 2,2′-dinitro-9,9′-spirobifluorene (**7**) in a regioselective manner. This approach not only allows introduction of the desired electron-withdrawing group but also regiospecifically drives the subsequent electrophilic bromi-

 © 2010 Wiley-VCH Verlag GmbH & Co. KGaA, Weinheim

nation towards the 7,7′-positions. As expected, the presence of the nitro groups prevents the formation of undesired by-products on phenyl rings that already bear nitro functions. 2,2′-Dibromo-7,7′-dinitro-9,9′-spirobifluorene (**8**) was thus obtained by reaction of **7** with bromine, in the presence of a catalytic amount of ferric chloride, in almost quantitative yield.

The synthesis of chromophores **1**–**5** is reported in Scheme 2. We were able to prepare compounds with a range of conjugation lengths through several palladium-catalyzed cross-coupling reactions between **8** and a suitable amino intermediate. In order to estimate the influence of the electronic connection between the acceptor and donor moieties in the spirobifluorene spacer itself, we synthesized 2,2′-dinitro-7,7′-dipiperidin-1-yl-9,9′-spirobifluorene (**1**) in 53% yield by Hartwig–Buchwald amination of **8** with piperidine, in the presence of Cs_2CO_3 as base and a combination of tris(dibenzylidenacetone)palladium [$Pd_2(dba)_3$] and tris-*tert*-butylphosphane ($PtBu_3$) as catalyst.

The application of Suzuki cross-coupling conditions, i.e., [$Pd(PPh_3)_4$] as catalyst and aqueous K_2CO_3 as base, provided an easy way to interpose a single phenyl ring between the donor and acceptor groups. The reaction of **8** with 4-(*N*,*N*-diphenylamino)phenyl boronic acid (**9**) afforded 2,2′-dinitro-7,7′-bis(4-*N*,*N*-diphenylaminophenyl)-9,9′ spirobifluorene (**2**) in 77% yield. Using the same synthetic procedure, the reaction of **8** and 4-(dimethylamino)phenyl boronic acid (**10**)[32] gave 2,2′-bis[4-(dimethylamino)phenyl]-7,7′-dinitro-9,9′-spirobifluorene (**3**) in 67% yield.

In addition to changing the electron-donating properties of the amino residue, we decided to introduce a double and a triple bond between the dimethylaminophenyl portion and the nitrospirobifluorene to verify the effect of increased conjugation length on the NLO properties. In particular, (*E*,*E*)-2,2′-bis{2-[4-(dimethylamino)phenyl]ethen-1-yl}-7,7′-dinitro-9,9′-spirobifluorene (**4**) was synthesized in 44% yield by Heck coupling between **8** and *N*,*N*-dimethyl-4-vinylaniline (**11**)[33] in anhydrous dimethylformamide

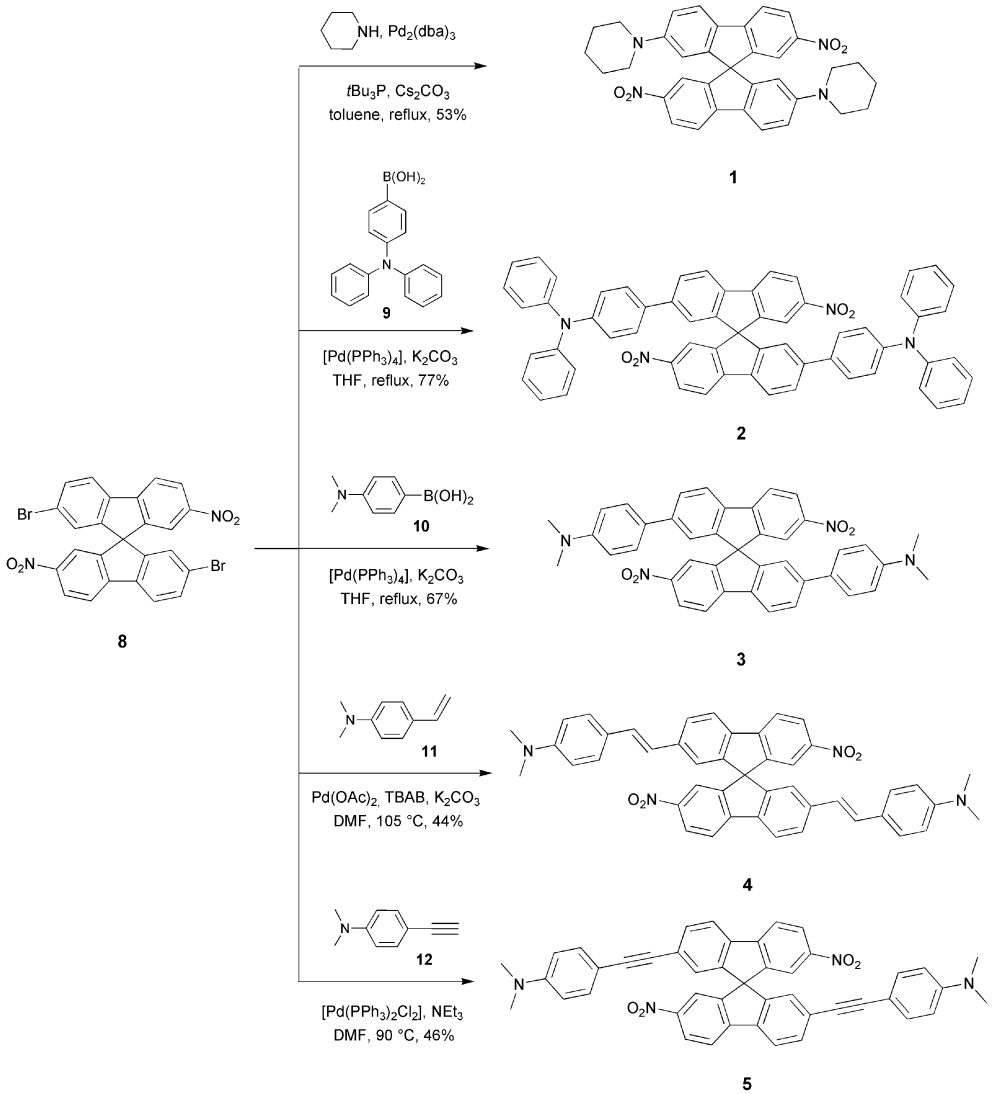

Scheme 2. Synthesis of push–pull spirobifluorenes **1**–**5**.

 © 2010 Wiley-VCH Verlag GmbH & Co. KGaA, Weinheim

(DMF) with $Pd(OAc)_2$ as catalyst and K_2CO_3 as base, in presence of tetrabutylammonium bromide (TBAB). We applied the Sonogashira coupling as described in the literature for different spirobifluorene derivatives[34] to generate 2,2′-bis{2-[4-(dimethylamino)phenyl]ethyn-1-yl}-7,7′-dinitro-9,9′-spirobifluorene (**5**) in 46% yield. The reaction was performed in anhydrous DMF between **8** and 4-ethynyl-*N*,*N*-dimethylaniline (**12**) by using bis(triphenylphosphane)palladium(II) dichloride $[Pd(PPh_3)_2Cl_2]$ as catalyst and triethylamine as base. In this case, the use of a copper salt as co-catalyst was not necessary, probably because of the very high reactivity of **12**.

To study the relationship between β and γ values and the number of chromophores present in the spiro system, we synthesized the corresponding monomers **1a**–**5a** through analogous synthetic pathways (Scheme 3). These compounds were prepared starting from 2-iodo-9,9-dimethyl-7-nitro-9*H*-fluorene (**13**),[35] which in turn was obtained by reaction of 2-iodo-7-nitro-9*H*-fluorene[36] with methyl iodide in dimethyl sulfoxide (DMSO) in the presence of KOH as base.

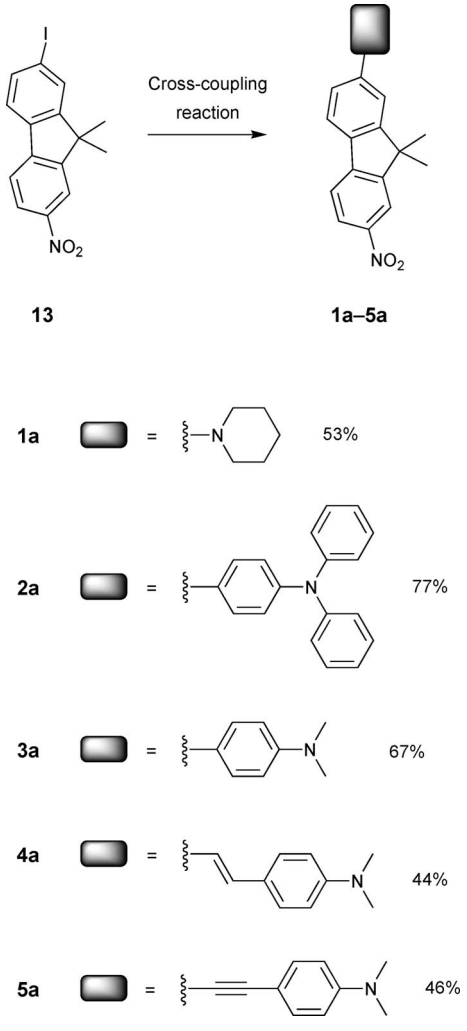

Scheme 3. Synthesis of push-pull fluorenes **1a**–**5a**.

Linear Optical Properties

To gain information on the electronic connection between donor and acceptor groups, experimental UV/Vis absorption spectra and time-dependent DFT (TDDFT) calculations of all compounds were performed. As reported in Figure 2, the absorption spectra of spirobifluorenes **1**–**5** in $CHCl_3$ solutions showed the presence of two broad bands, one lying in the UV region (270–325 nm) that can be attributed to π–π* transitions and another at lower energy (410–438 nm) assigned to charge-transfer transitions (CT).

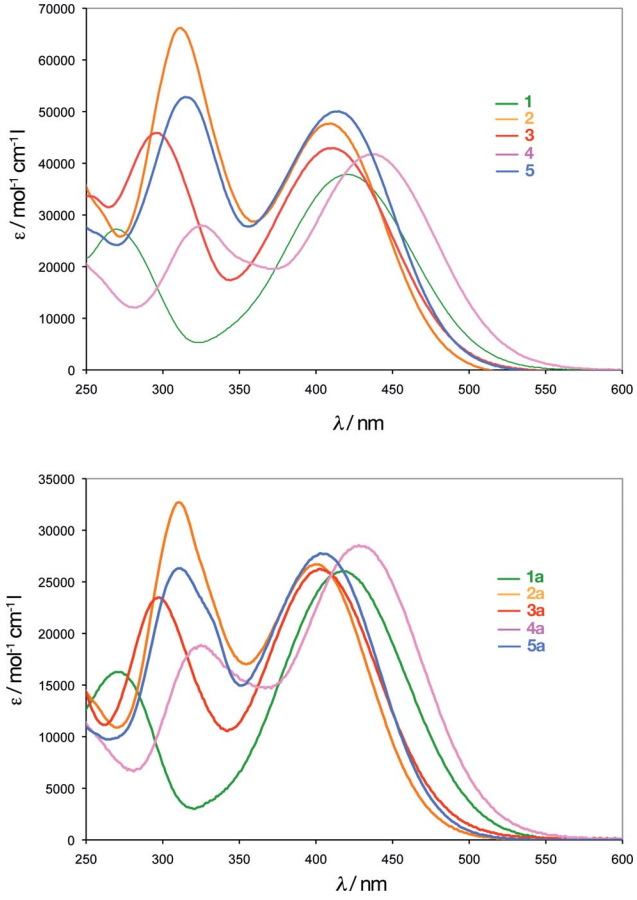

Figure 2. Absorption profiles of spirobifluorenes **1**–**5** (top) and fluorenes **1a**–**5a** (bottom).

The absorption maxima wavelengths of **1** coincides with that of the reference monomer **1a** (Table 1). Replacement of the piperidinyl donor groups with triphenylamines in spirobifluorene **2** and fluorene **2a** leads to a hypsochromic shift of the CT absorption band together with a bathochromic shift of the π–π* maximum.

Moving from **2** to **3**, substitution of the phenyl moiety with alkyl residues should increase the electron density on the nitrogen atom through an inductive effect. At the same time, the electron density at the nitrogen should be reduced by loss of resonance delocalization on the missing phenyl groups.[39] The net effect we observed by changing the donor properties of the amine substituents in **3** and **3a**, is an unperturbed charge-transfer band compared to **2** and **2a**. Conversely, a significant decrease in the intensity of the π–

 © 2010 Wiley-VCH Verlag GmbH & Co. KGaA, Weinheim

Table 1. Experimental and computed absorption maxima of push–pull fluorene (**1a**–**5a**) and spirobifluorene (**1**–**5**) derivatives.

Compound	λ_{exp} [nm][a]	ε [L cm^{-1} mol^{-1}][a]	λ_{theor} [nm][b]
1a	272, 418	16100, 25800	249, 373
1a′			251, 393
1	270, 420	27800, 38700	248, 378
1′			252, 396
2a	311, 401	31700, 25800	303, 388
2	311, 410	64400, 46400	303, 397
3a	297, 403	23300, 26100	286, 387
3	297, 410	40900, 42600	279, 394
4a	325, 428	18300, 27900	320, 426
4	325, 438	29200, 43800	322, 434
5a	311, 403	26400, 27700	303, 404
5	315, 415	52400, 49600	306, 413

[a] $CHCl_3$ solutions. [b] Simulated TDDFT absorption bands calculated by using MPW1K[37] functional, including solvation effects ($CHCl_3$) by the conductor polarizable continuum model (C-PCM) as implemented in G03.[38]

π* band and its displacement to higher energies were measured. Absorption profiles of spiro-compound **4** and fluorene **4a**, which both have an additional double bond linker, showed a bathochromic shift of 25 nm for the π–π* band and of 28 nm for the CT band, reflecting the increased conjugation. Finally, the replacement of a double bond in **4** and **4a** with a triple bond spacer in **5** and **5a** leads to a blueshift of both the CT and π–π* bands.

In addition to these spectroscopic details, two more important observations can be noted. With the exception of the pair **1** and **1a**, a slight bathochromic displacement (7–12 nm) of the CT maxima bands was measured for spirobifluorenes **2**–**5**. Although these spectral shifts are small enough to suggest the presence of quasi-independent active chromophores, the scaling of absorptive properties passing from compounds **1**–**5** to **1a**–**5a** does not completely agree with this hypothesis. In fact, the ratio of molar extinction coefficients between the spiro-compounds and the reference fluorenes is less than 2 in most cases. This result can be interpreted as an indication of some weak interaction taking place between the two molecular halves of **1**–**5**.

Quantum mechanical calculations were performed to characterize the excited states and the electronic transitions giving rise to the absorption bands of both push–pull fluorenes and spirobifluorenes spectra.

The DFT-optimized molecular structures of all spirobifluorenes show that the two halves are essentially mutually orthogonal, being characterized by a dihedral angle between the planes containing the two fluorene units that varies from 89.0° for **1** to 88.4° for **4**. The optimized geometrical parameters do not significantly vary on passing from the fluorene to the spirobifluorene systems, where a slight lengthening by 0.02 Å is found for the C–C bonds involving the spiro center in the spirobifluorene derivatives and a decrease of the related angle by ca. 2° is computed.

Interestingly, for fluorene **1a** and spiro-compound **1**, two minima were found according to the conformation adopted by the piperidine, the chair form being more stable by approximately 4 and 3 kcal/mol, respectively, than the half-chair piperidine conformation (hereafter labelled **1a′** and **1′**).

The frontier molecular orbital energies and HOMO and LUMO isodensity plots of all investigated fluorene **1a**–**5a** derivatives are reported in Figure 3. It is worth noting that the energy of the LUMOs is quite similar, being only slightly lower in the case of compounds **2a**, **4a**, and **5a**. The

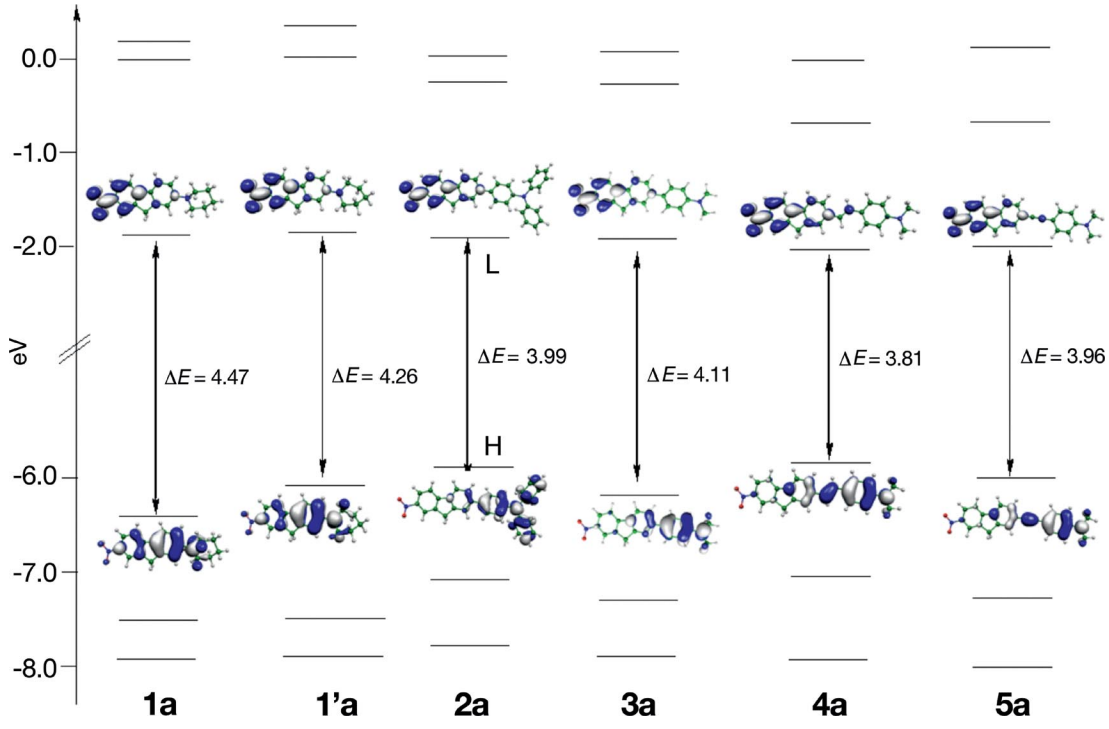

Figure 3. Frontier orbital energies of the fluorene compounds **1a**–**5a**. The isodensity plot of HOMOs and LUMOs are reported.

 © 2010 Wiley-VCH Verlag GmbH & Co. KGaA, Weinheim

character of the LUMOs is also very similar along the series, with the electronic charge delocalized on the acceptor part of the molecule with a different involvement of the fluorene core. On the other hand, the HOMO reflects the different donor substituents on the investigated compounds and shows a different charge delocalization. In particular, the HOMOs are delocalized on the donor moiety of the fluorenes for **2a**–**5a**, whereas they show a contribution within the fluorene unit for **1a** and **1a**′. The HOMO energies for all the compounds show a higher variability, lying in the range of 5.7–6.3 eV. The HOMO of **1a** (**4a**) is the most stabilized (destabilized), and the HOMO–LUMO gap energies (ΔE_{H-L}) are directly affected by the position of the HOMO. Indeed, the largest and the smallest ΔE_{H-L} were computed to be 4.37 and 3.81 eV for **1a** and **4a**, respectively, which reflects the stronger donor ability of the NMe_2 fragment connected to the fluorene moiety by a C=C double bond.

Notably, a general trend can be seen upon going from the monomers to the spiro-dimers, which can be exemplified by comparing the electronic structures of **3a** and **3**. As already mentioned, the HOMO of **3a** is localized on the dimethylaniline − the donor part of the molecule − whereas the LUMO is localized on the acceptor part. In the spirobifluorene compound **3**, the π orbitals of the monomer moieties combine in a symmetric and anti-symmetric way to provide two almost degenerate orbitals (Figure 4). The HOMO–LUMO gap only slightly reduces on passing from **3a** to **3** (4.11 eV/4.04 eV), mainly by virtue of a LUMO stabilization. In all cases, the electronic structure of the spiro-dimers can be described as pairs of orbitals, which are the bonding/antibonding combination of the corresponding monomer orbitals. They are delocalized in the two substituted fluorene units and possess similar energy with respect to the corresponding monomer orbitals. In general, on passing from the fluorene to the spirobifluorene systems, we did not observe the spiro-conjugation coupling for the HOMO; the computed spirobifluorene HOMO and

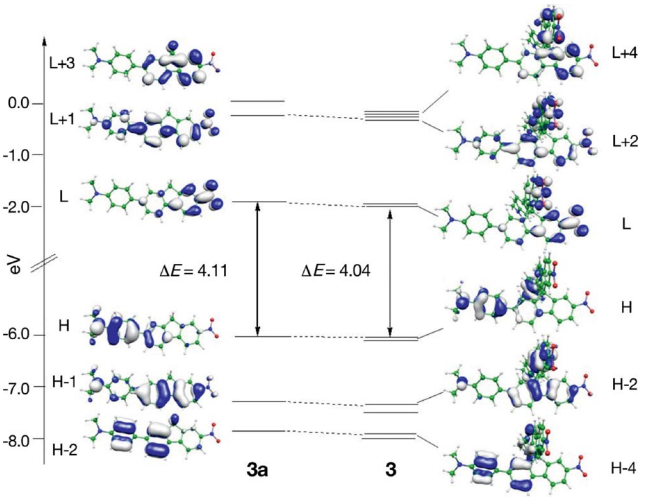

Figure 4. Molecular orbital energies of **3a** and **3**. The isodensity plots of selected orbitals are reported.

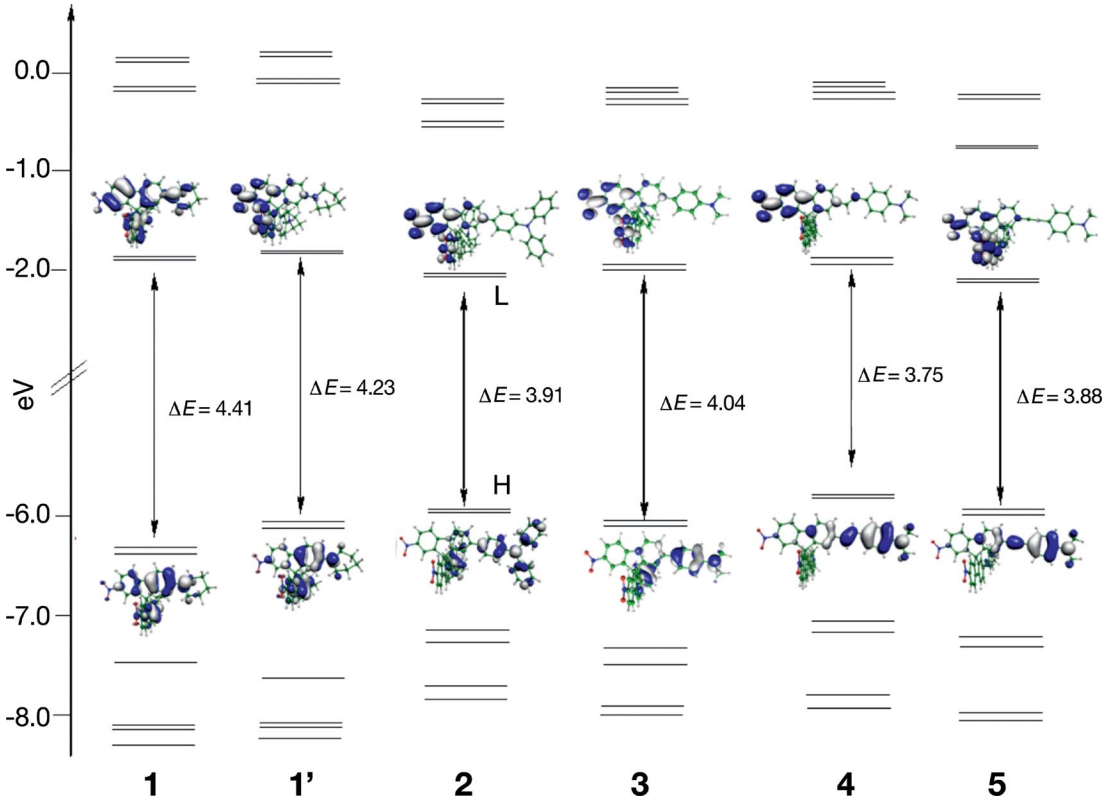

Figure 5. Frontier orbital energies of the fluorene compounds **1**–**5**. The isodensity plot of HOMOs and LUMOs are reported.

 © 2010 Wiley-VCH Verlag GmbH & Co. KGaA, Weinheim

HOMO-1 orbitals were almost degenerate and had essentially the same energy with respect to the fluorene HOMO. This is due to the character of the fluorene HOMO, which shows negligible electron density on the atoms adjacent to the spiro carbon. On the other hand, the monomer HOMO-1 is mainly localized on the fluorene moiety. In the dimer the correspondig orbitals, HOMO-2 and HOMO-3, are split by virtue of the spiro-conjugation.[40,41] In Figure 5, the frontier molecular orbital energies with HOMO and LUMO isodensity plots of all the spirobifluorene derivatives **1**–**5** are reported. In line with the discussion above, the ΔE_{H-L} decreases from the fluorene to the spirobifluorene for **1**′ and **2**–**5** compounds, which is essentially due to a stabilization of the LUMO; a fact that partly justifies the bathochromic shift of the CT band of the spirobifluorenes spectra.

The overall picture of the molecular frontier orbitals of the spirocompounds describes a partial coupling that occurs between the two orthogonal units, a fact that has implications on the nonlinear optical properties. We then simulated the UV/Vis spectra of all the investigated systems and analyzed the computed TDDFT eigenvalues and eigenvectors. The absorption band maxima of the simulated TDDFT spectra are compared with the experimental values in Table 1. As an example, the calculated absorption spectra of **3a** and **3** are reported in Figure 6. We computed that the lowest absorption band of **3a** at 387 nm originated from a single transition of charge-transfer (CT) character from the HOMO to the LUMO. This computed band is blueshifted compared to the experimental value (403 nm). With reference to the results obtained with **3a**, the experimental absorption band at 297 nm has been computed to occur at 286 nm and originates essentially from two transitions at 294 nm ($f = 0.26$) and 275 nm ($f = 0.45$), involving the lower lying HOMOs and the LUMO/LUMO+1. The former transition, therefore, has the π orbital delocalized on the fluorene unit of the **3a** compound in the starting state and the π* orbital on the acceptor part of the molecule in the arriving state. The main contribution of the latter transition is represented by a transition within the acceptor part of the molecule, i.e., from the phenyl ring to the nitro group.

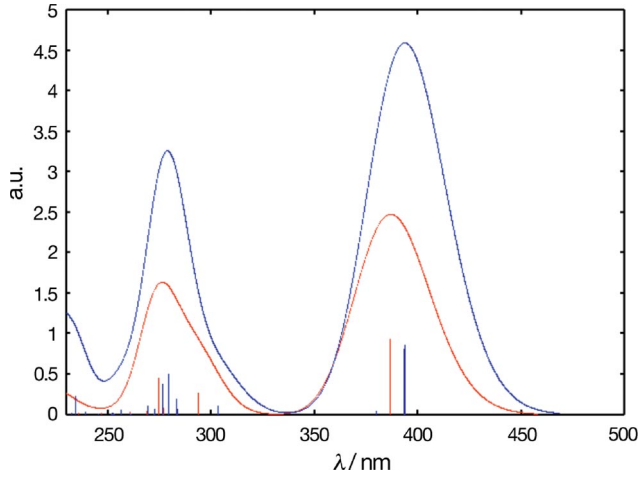

Figure 6. Simulated absorption spectra of **3a** (red) and **3** (blue); MPW1K data in solution.

For spirobifluorene **3**, the lowest absorption band is slightly redshifted with respect to that of the monomer **3a**, being centered at 394 nm (3.15 eV) for the former versus 387 nm (3.21 eV) for the latter, the same trend was observed experimentally, with maxima at 410 nm (3.03 eV) and 403 nm (3.08 eV), respectively.

As can be seen, apart from a quasi-rigid blueshift of the calculated data of approximately 0.15 eV, the small shift of the absorption band going from **3a** to **3** is nicely reproduced. It is worth noting that in the case of **3**, the lowest absorption band originates from two degenerate CT transitions of comparable intensity involving the HOMO/LUMO+1 and the HOMO–1/LUMO excitations. These transitions dominate the (second order) NLO response of the investigated systems, which is expected to slightly increase compared to the monomer by virtue of the lower energy excitation, at only little expense to the optical transparency.

The spectra of all the spirobifluorene compounds show the same trends, which can be seen in Table 1 as a comparison between theory and experiment. The calculated spectra of compounds **5a**, **5**, **4a**, and **4** are in excellent agreement with the experimental values. Deviations within 0.2 eV are calculated for the other chromophores, with compounds **1** and **1a** showing the largest blue-shifts compared to the experimental data. This is possibly due to the influence of dynamic effects on the calculated spectra, as suggested by the sensitivity of the calculated data to the selected piperidine conformation.

Nonlinear Optical Properties

The molecular NLO responses of the push–pull spirobifluorene derivatives **1**–**5** and those of the corresponding monomers are reported in Table 2. All compounds were measured in liquid solution by the direct current electric-field-induced second-harmonic (EFISH) generation method,[42–44] which can provide γ_{EFISH} values, that is, direct information on the molecular NLO properties, by using Equation 1.

$$\gamma_{EFISH} = \frac{\mu\beta_\lambda}{5kT} + \gamma_0(-2\omega;\ \omega,\ \omega,\ 0) \quad (1)$$

$\mu\beta_\lambda/5kT$ is the dipolar orientational contribution, with β_λ being the projection along the dipole moment axis of the vectorial component β_{VEC} of the quadratic hyperpolarizability tensor, μ is the static dipole moment, ω is the fundamental wavelength of the incident photon, and $\gamma_0(-2\omega;\ \omega,\ \omega,\ 0)$, which is a third-order term at frequency ω of the incident light, is the cubic electronic contribution to γ_{EFISH}. The values of $\mu\beta_\lambda$ were directly obtained from the EFISH measurement by considering the γ_0 contribution to γ_{EFISH} to be negligible. The purely electronic cubic hyperpolarizabilities, $\gamma_{THG}(-3\omega;\ \omega,\ \omega,\ \omega)$, were measured by third harmonic generation (THG) experiments.

 © 2010 Wiley-VCH Verlag GmbH & Co. KGaA, Weinheim

Table 2. Experimental and calculated molecular NLO properties of push–pull fluorenes and spirobifluorene derivatives.

	γ_{EFISH} [$\times 10^{-34}$ esu][a]	γ_{THG} [$\times 10^{-34}$ esu][a]	μD[b]	$\mu\beta_\lambda$ [$\times 10^{-48}$ esu][a]	μ_{theor} [D]	β_{theor} [$\times 10^{-30}$ esu][c]	$\beta_{yyy\ theor}$ [$\times 10^{-30}$ esu][c]	$\beta_{zzz\ theor}$ [$\times 10^{-30}$ esu][c]	$\mu\beta_{theor}$ [$\times 10^{-48}$ esu]
1a	1.75	2.59	4.2	342	9.8	43			421
					11.6	57			661
2a	1.65	2.70	3.3	325	8.3	65			540
3a	1.90	3.30	5.9	355	10.6	65			689
4a	1.40	3.10	2.1	270	11.9	138			1642
5a	1.35	3.05	4.2	250	11.4	109			1243
1	2.48	8.89	4.4	567	13.9	59	41	43	820
1′					16.2	76	54	53	1231
2	2.91	9.63	6.6	600	11.8	103	73	72	1215
3	1.89	12.88	6.9	390	14.8	98	69	69	1450
4	4.20	11.00	5.3	850	16.6	208	148	146	3453
5	3.90	10.71	4.7	800	16.2	173	121	123	2803

[a] In $CHCl_3$ solutions at the same concentration (10^{-3} M) working at a nonresonant incident wavelength of 1.907 μm. [b] Determined in anhydrous $CHCl_3$ by the Guggenheim method.[47,48] [c] Calculated by a combined Finite Fields and Coupled Perturbed Kohn Sham formalism as implemented in G03, in which numerical differentiation of analytic polarizabilities in the presence of an external electric field is performed.

The γ_{EFISH} and $\mu\beta_\lambda$ values of fluorene derivatives **1a**–**5a** (Table 2) are very similar, and a clear trend cannot be inferred, especially considering that the difference between consecutive values is less than the experimental error of the EFISH measurement, which allows the values to be estimated with a standard deviation in the order of 10–15%. However, taking into account the data obtained for spirobifluorenes **1**–**5**, a trend can be observed that could be explained on the basis of theoretical considerations of the conjugation allowed by the spacers involved. As other authors suggested,[45] the enhancement in hyperpolarizability upon going from **1** and **3** to **2** can be interpreted on the basis of the larger perturbation in the energy of the donor orbital by the phenyl substituent and on the additional contribution of π-electron density from the phenyl, as also confirmed by the observed decrease of ΔE_{H-L}. Since a double bond is superior to a triple bond in transmitting charge from the donor to the acceptor moieties,[46] the improved electronic communication along the series **4** → **5** → **3** finds its counterpart in the increased values of $\mu\beta_\lambda$.

Particularly interesting are the experimental results on the purely electronic cubic hyperpolarizabilities γ_{THG}. In the hypothesis of no electronic coupling between two monomer units, the γ value of a dimer can be related to that of a monomer by Equation 2.[26]

$$\langle\gamma\rangle_{spiro} = \langle\gamma\rangle_{monomer} \times 4(1 + \cos\vartheta)^2 \quad (2)$$

ϑ is the dihedral angle between two dipoles. Thus, when ϑ is approximately 90° for spirobifluorene derivatives, a $\gamma_{THGspiro}/\gamma_{THGmonomer}$ ratio equal to 4 is expected. Our experimental results give a very reproducible ratio that always falls in the interval 3.43–3.9.

Although a substantial increase of $\mu\beta_\lambda$ was measured for our spiro-compounds with respect to the corresponding fluorene (with the exception of the pair **3a/3**), the analysis of experimental dipole moments and the quadratic hyperpolarizability values is less straightforward. In order to provide a rationale for the nonlinear optical properties of fluorenes and related spirobifluorene, we have computationally investigated the ground-state dipole moment, the static hyperpolarizability, and $\mu\beta_\lambda$, which is experimentally observable, of all the investigated systems.

In Table 2, the computed ground-state dipole moments of fluorenes and spirobifluorenes under study are reported. The calculated dipole moment of all the investigated fluorenes originated from a charge asymmetry from the partly negatively charged NO_2 ligand, which prevails over donation from the disubstituted amine ligand, similar to the *para*-nitroaniline case. The dipole moments of the monomers are in the range of 8.3–11.9 D, and they essentially coincide with the value of their z component, i.e., they were oriented along the main molecular axis. The dipole moments of the spirobifluorene derivatives are increased compared to the monomers, with values in the range of 11.8–16.6 D. As expected, the dipole is the resulting vector of the two almost equivalent μ_y and μ_z components, which are characterized by a similar value and the same direction as those of the monomers. Overall, we observe that the dipole moment of the investigated spirobifluorene is essentially equal to $\mu_{spiro} = [\cos(\pi/4) \times (\mu_y + \mu_z)]$, it therefore crosses the spiro region and is directed between the two $-NR_2$ ends. The comparison between the calculated and experimental values shows a general overestimation of calculated dipole moments, although the experimental trends are roughly reproduced considering that the dipole moments of all compounds are quite similar and that an increase is observed passing from the fluorenes to the related spirobifluorenes. As excited states, the absolute values of these results are clearly sensitive to the level of theory and therefore to the xc functional employed. Nevertheless, the same conclusion holds for the trends going from the monomer to the spirodimer, independent of the xc functional used and whether the calculations involved in vacuo or solution methods. Actually, the measured dipole moments for **2a** and **4a** were surprisingly low.

 © 2010 Wiley-VCH Verlag GmbH & Co. KGaA, Weinheim

The calculated static hyperpolarizabilities β of the investigated fluorene series are reported in Table 2 together with $\mu\beta$ values. The obtained values are in satisfactory agreement with the experimental data, taking into account the general overestimation of the theoretical values due to the computed dipole moments. We notice, however, that a direct comparison between the theoretical and experimental data is not straightforward due to the neglect in the former of the dispersion and vibrational contribution to the second-order NLO response.

For the spirobifluorenes, analogously to the calculations on the dipole moment, the only relevant components of the β tensor are β_{yyy} and β_{zzz}, which are almost equivalent and correspond to the β components along the z and y axes of the dipole moments. We therefore evaluated the values of β using the following equation: $\beta = [\cos(\pi/4)\ (\beta_{yyy} + \beta_{zzz}) \times 10^{-48}$ esu]. The values of the two spirobifluorenes hyperpolarizability components are related to the monomer values, and show an increase with respect to the value of the corresponding fluorene directly depending on the rigid conformation of the spiro-compounds. Looking at the theoretical $\mu\beta$ values, analogously to the fluorene case, we observe a general overestimation with respect to the EFISH measurements, which is again due to the overestimated dipole moments. However, with the exception of **3**, a reasonable correlation between theory and experiment is observed. Overall, some general trends can be drawn within the spirobifluorene series. In particular, it is interesting that a relationship can be found between the NLO behavior and the optical properties among the series **3**→**4**→**5**. The (dimethylamino)phenyl donor group in **3** is connected directly to the spiro moiety, whereas in **4** and **5** a double and triple bond spacer, respectively, is inserted between the donor group and the spirobifluorene moiety. Along this series, both the monomer and dimer NLO response follow the trends in HOMO–LUMO and lowest transition energies, which is in line with the two-level model, which predicts that the hyperpolarizability will increase as the transition energies decrease. The effect of the conjugate spacer induces a substantial increase in the NLO response of both the monomers and dimers. Besides the transition red-shift already mentioned, this effect is also due to the higher polarizability introduced in the molecules by the conjugated spacers. Changing a double bond to a triple bond as spacer implies a decrease of the NLO response, due to the smaller conjugating ability of the triple bond.[46]

It is also interesting to analyze the effect of replacing the methyl substituents in **3** with phenyl substituents in **2**. This substitution, which does not have any impact on the NLO response of the fluorene monomers (65×10^{-30} esu for both **2a** and **3a**), slightly affects the computed hyperpolarizability of the spirobifluorenes, with the increase related to the presence of the phenyl substituents. This increase comes at basically no cost to transparency, because both species show essentially the same absorption maxima. This interesting observation, which is possibly due to the polarizable nature of the phenyl substituents, can offer additional guidance for future design strategies aimed at increasing the NLO response without compromising the optical transparency.

Conclusions

A new class of push–pull chromophores with disubstituted amine as donor and nitro group as acceptor connected to a spirobifluorene core has been synthesized. A simple synthetic approach was employed to obtain geometrically oriented push–pull bichromophoric systems and the corresponding push–pull fluorene monomers with good yields. Using electric field second harmonic and third harmonic generation methods, the nonlinear optical properties of spirobifluorene derivatives have been experimentally investigated for the first time. Furthermore, we compared the first and second hyperpolarizability (β and γ) of the spiro-compounds with the corresponding fluorene monomers. We found that the first hyperpolarizability β is enhanced on passing from the monomer to the corresponding spiro-dimer without substantial variation of the maximum of the absorption bands. Particularly interesting are the experimental results on the γ_{THG}. In fact, the ratio $\gamma_{THGspiro}/\gamma_{THGmonomer}$ is expected to be equal to 4[26] and our experiments have given very reproducible data that was always in the range 3.43–3.9.

By calculating the optimized molecular structures and conducting subsequent analyses of the electronic structure of all compounds, the HOMO levels were found to be localized on the donor part of the molecule and reflected the different donor substituents, whereas the LUMOs were found to be quite similar, with the electronic charge being delocalized on the nitro group and the adjacent phenyl ring. Remarkably, the electronic structure of the spirobifluorene compounds can be described as pairs of orbitals that are delocalized on the two molecular halves and which are at similar energy with respect to the corresponding monomer orbitals; this fact has a large impact on the related linear and nonlinear optical properties of the spiro-derivatives compared to the fluorenes. In fact, the computed lowest energy band of the spirobifluorene UV/Vis spectra originates from two equivalent CT transitions, each one taking place in a fluorene unit.

The first hyperpolarizability β of the spirobifluorene has been computed to arise as a result of the two almost equivalent components (β_{yyy} and β_{zzz}) along the dipole moments z and y axes, thus confirming the experimentally observed increase in the dipole moment of the spiro-dimer compared to the fluorene. Moreover, analysis of the spirobifluorene series **3/4/5**, in which a double or triple bond is inserted between the donor group and the spirobifluorene core, revealed a significant increase in the β values. Finally, substitution of the dimethylamine **3** with the diphenylamine **2** results in a sizeable enhancement of the first hyperpolarizability, which can be ascribed to a "non-traditional" π-conjugation effect as described in the literature.[37,45]

This study covers a number of spirobifluorene compounds that have not previously been fully investigated. The

 © 2010 Wiley-VCH Verlag GmbH & Co. KGaA, Weinheim

geometrically rigid structure of these bichromophoric systems could be used as a base from which to design molecular materials with high NLO properties without significant modifications to the optical behavior of the single chromophore.

Experimental Section

General: All commercially available solvents and reagents were used as received without further purification. 2,2′-Dinitro-9,9′-spirobifluorene (**7**),[31] 4-(dimethylamino)phenylboronic acid (**10**),[32] *N*,*N*-dimethyl-4-vinylaniline (**11**),[33] 2-iodo-7-nitro-9*H*-fluorene,[36] and 2-iodo-9,9-dimethyl-7-nitro-9*H*-fluorene (**13**)[35] were synthesized according to literature procedures. Coupling reactions were performed under nitrogen using standard Schlenk techniques. Thin layer chromatography (TLC) was performed on plates precoated with silica gel Si60-F254 (Merck, Darmstadt, Germany). Column chromatography was carried out with silica gel Si60, mesh size 0.040–0.063 mm (Merck, Darmstadt, Germany). Flash chromatography was carried out on silica gel, mesh size 230–400 (J. T. Baker). ^{1}H and ^{13}C NMR spectra were recorded with a Bruker Avance 400 (400 and 100.6 MHz, respectively) spectrometer. Chemical shifts are indicated in parts per million downfield from $SiMe_4$, using the residual proton ($CHCl_3$ δ = 7.26 ppm) and carbon ($CDCl_3$ δ = 77.0 ppm) solvent resonances as internal reference. The coupling constants *J* are given in Hz. Proton and carbon atom assignments were determined by performing COSY and HSQC correlation experiments. ESI mass spectra were obtained with an electrospray ion-trap mass spectrometer ICR-FTMS APEX II (Bruker Daltonics) by the Centro Interdipartimentale Grandi Apparecchiature (C.I.G.A.) of the University of Milano. Melting points were determined with a Büchi Melting Point B-540 capillary melting point apparatus. UV/Vis spectra were recorded with a Nicolet Evolution 500 (Thermo Electron Corporation) spectrometer. All EFISH and THG measurements were carried out in $CHCl_3$ solutions at the same concentration (10^{-3} M) working at a nonresonant incident wavelength of 1.907 μm, using a Q-switched, mode-locked Nd^{3+}:YAG laser manufactured by Atalaser equipped with a Raman shifter; the apparatus used for the EFISH measurements was made by SOPRA (France). All experimental EFISH β_λ values are defined according to the "phenomenological" convention.[49] Dipole moments μ were determined in anhydrous $CHCl_3$ by the Guggenheim method.[47,48]

Theoretical Calculations: The molecular structure of all fluorenes **1a**–**5a** and related spirobifluorenes **1**–**5** were optimized using a 6-31g** basis set[50] and B3LYP exchange-correlation functional[51] in vacuo, without any symmetry constraints, by using the Gaussian03 (G03) program package.[52] On all the optimized molecular geometries, the analysis of the electronic structure and Time-Dependent DFT (TDDFT) calculations were performed using the 6-31g** basis set, and the hybrid B3LYP and MPW1K[38] functionals and included the solvation effects by the conductor polarizable continuum model (C-PCM) as implemented in G03.[39] The MPW1K functional was chosen because, due to increased amounts of Hartree–Fock exchange, the results were particularly effective in accurately describing the charge transfer systems.[38,53] The lowest 20 (60) TDDFT singlet–singlet excitations for all the monomers (dimers) were computed. To simulate the absorption spectra, thus allowing a direct comparison with the experimental data, the computed transition energies and oscillator strengths were convoluted by Gaussian functions with a σ of 0.2 eV. The static quadratic hyperpolarizability β were calculated by a combined Finite Fields and Coupled Perturbed Kohn Sham formalism as implemented in G03, in which numerical differentiation of analytic polarizabilities in the presence of an external electric field was performed.

2,2′-Dibromo-7,7′-dinitro-9,9′-spirobifluorene (8): Bromine (1 mL, 19.52 mmol) was added dropwise to a stirred solution of **7** (1.87 g, 4.61 mmol) and anhydrous $FeCl_3$ (40 mg, 0.247 mmol) in CH_2Cl_2 (45 mL). The mixture was refluxed for 5 h and then cooled to r.t. The solution was washed with saturated $NaHCO_3$ (2 × 30 mL), saturated $Na_2S_2O_3$ (2 × 30 mL) and water (2 × 30 mL). The organic layer was dried with Na_2SO_4 and the solvent was removed under vacuum to give **8** (2.54 g, > 95%) as a pale-yellow solid; m.p. 360–365 °C. ^{1}H NMR (400 MHz, $CDCl_3$, 25 °C): δ = 8.37 (dd, $J_{H,H}$ = 8.5, $J_{H,H}$ = 2.1 Hz, 2 H, 6-H, 6′-H), 8.00 (d, $J_{H,H}$ = 8.5 Hz, 2 H, 5-H, 5′-H), 7.85 (d, $J_{H,H}$ = 8.2 Hz, 2 H, 4-H, 4′-H), 7.66 (dd, $J_{H,H}$ = 8.2, $J_{H,H}$ = 1.8 Hz, 2 H, 3-H, 3′-H), 7.56 (d, $J_{H,H}$ = 2.1 Hz, 2 H, 8-H, 8′-H), 6.91 (d, $J_{H,H}$ = 1.7 Hz, 2 H, 1-H, 1′-H) ppm. ^{13}C NMR (101 MHz, $CDCl_3$, 25 °C): δ = 149.41 (q), 147.99 (q), 147.23 (q), 146.88 (q), 138.32 (q), 132.72 (6-C, 6′-C), 127.63 (8-C, 8′-C), 125.12 (3-C, 3′-C), 124.58 (q), 123.25 (5-C, 5′-C), 120.99 (4-C, 4′-C), 119.65 (1-C, 1′-C), 65.18 (9-C) ppm. HRMS (ESI+): calcd. for $C_{25}H_{12}N_2O_4Br_2$ $[M + H]^+$ 563.9140; found 563.9144. $C_{25}H_{11}Br_2N_2O_4$ (563.17): calcd. C 53.22, H 2.14, N 4.97; found C 53.35, H 2.14, N 4.98.

2,2′-Dinitro-7,7′-di(piperidin-1-yl)-9,9′-spirobifluorene (1): In a Schlenk tube, a solution of $Pd_2(dba)_3$ (22 mg, 0.024 mmol) and P*t*Bu$_3$ (1 M in toluene, 40 μL, 0.04 mmol) in anhydrous toluene (2 mL) was stirred at r.t. for 20 min. The mixture was transferred by using a cannula to a second Schlenk tube containing a suspension of **8** (250 mg, 0.445 mmol), Cs_2CO_3 (510 mg, 1.566 mmol), and piperidine (108 μL, 1.092 mmol) in anhydrous toluene (4 mL). The mixture was heated to reflux under vigorous stirring for 24 h. After cooling to r.t., saturated NH_4Cl (10 mL) was added and the mixture was extracted with ethyl acetate (4 × 15 mL). The collected organic phases were dried with Na_2SO_4 and the solvent was removed under vacuum. The crude material was purified by flash chromatography (hexane/ethyl acetate, 9:1) to give **1** (135 mg, 53%) as a red solid; m.p. 175–195 °C. ^{1}H NMR (400 MHz, $CDCl_3$, 25 °C): δ = 8.26 (dd, $J_{H,H}$ = 8.5, $J_{H,H}$ = 2.0 Hz, 2 H, 3-H, 3′-H), 7.78 (d, $J_{H,H}$ = 8.6 Hz, 2 H, 5-H, 5′-H), 7.77 (d, $J_{H,H}$ = 8.5 Hz, 2 H, 4-H, 4′-H), 7.47 (d, $J_{H,H}$ = 2.1 Hz, 2 H, 1-H, 1′-H), 7.0 (dd, $J_{H,H}$ = 8.6, $J_{H,H}$ = 1.8 Hz, 2 H, 6-H, 6′-H), 6.97 (d, $J_{H,H}$ = 1.9 Hz, 2 H, 8-H, 8′-H), 3.11–3.09 (m, 8 H, piperidine), 1.60–1.50 (m, 12 H, piperidine) ppm. ^{13}C NMR (101 MHz, $CDCl_3$, 25 °C): δ = 153.85 (q), 150.99 (q), 148.88 (q), 148.34 (q), 146.09 (q), 129.66 (q), 124.69 (3-C, 3′-C), 122.53 (4-C, 4′-C), 119.35 (1-C, 1′-C), 118.75 (5-C, 5′-C), 115.96 (6-C, 6′-C), 110.48 (8-C, 8′-C), 65.51 (9-C), 49.60 (2-C piperidine, 6-C piperidine), 25.57 (3-C piperidine, 5-C piperidine), 24.05 (4-C piperidine) ppm. UV/Vis ($CHCl_3$): λ_{max} (ε, $mol^{-1}\,dm^3\,cm^{-1}$) = 270 (27800), 420 (38700) nm. HRMS (ESI+): calcd. for $C_{35}H_{33}N_4O_4$ $[M + H]^+$ 573.2496; found 573.2484. $C_{35}H_{32}N_4O_4$ (572.65): calcd. C 73.41, H 5.63, N 9.78; found C 73.55, H 5.64, N 9.77.

7,7′-Bis[4-(diphenylamino)phenyl]-2,2′-dinitro-9,9′-spirobifluorene (2): In a Schlenk tube, a stirred mixture of **8** (112 mg, 0.198 mmol), boronic acid **9** (233 mg, 0.806 mmol), aqueous K_2CO_3 (1 M, 2.4 mL, 2.4 mmol), and $Pd(PPh_3)_4$ (12 mg, 0.011 mmol) in anhydrous THF (5 mL) was refluxed overnight under an inert atmosphere. After cooling to r.t., THF was removed under vacuum and the aqueous phase was extracted with CH_2Cl_2 (3 × 20 mL). The collected organic phases were dried with Na_2SO_4 and the solvent was removed under vacuum. The crude material was purified by column chromatography over silica (hexane/ethyl acetate, 5:1) to

 © 2010 Wiley-VCH Verlag GmbH & Co. KGaA, Weinheim

give the product **2** (137 mg, 77%) as an orange solid; m.p. 195–197 °C. ^{1}H NMR (400 MHz, $CDCl_3$, 25 °C): δ = 8.35 (dd, $J_{H,H}$ = 8.4, $J_{H,H}$ = 2.0 Hz, 2 H, 3-H, 3′-H), 8.01 (d, J_{H-H} = 8.1 Hz, 2 H, 5-H, 5′-H), 8.00 (d, J_{H-H} = 8.4 Hz, 2 H, 4-H, 4′-H), 7.72 (dd, J_{H-H} = 8.0, J_{H-H} = 1.2 Hz, 2 H, 6-H, 6′-H), 7.60 (d, J_{H-H} = 1.9 Hz, 2 H, 1-H, 1′-H), 7.31 (d, J_{H-H} = 8.6 Hz, 4 H, Ph-H), 7.24–7.21 (m, 8 H), 7.07–6.98 (m, 16 H) ppm. ^{13}C NMR (101 MHz, $CDCl_3$, 25 °C): δ = 149.28 (q), 148.53 (q), 148.02 (q), 147.87 (q), 147.50 (q), 147.36 5 (q), 143.13 (q), 137.97 (q), 133.48 (q), 129.31 (Ph), 127.81 (2-C phenyl-spiro, 6-C phenyl-spiro), 127.59 (6-C spiro), 124.80 (3-C spiro), 124.58 (Ph), 123.38 (Ph), 123.24 (Ph), 122.23 (5-C, 5′-C, 8-C, 8′-C), 120.52 (4-C, 4′-C), 119.62 (1-C, 1′-C), 65.71 (9-C) ppm. UV/Vis ($CHCl_3$): λ_{max}(ε, mol^{-1} dm^3 cm^{-1}) = 311 (64400), 410 (46400) nm. HRMS (ESI+): calcd. for $C_{61}H_{41}N_4O_4$ $[M + H]^+$ 893.3122; found 893.3149. $C_{61}H_{40}N_4O_4$ (892.99): calcd. C 82.04, H 4.51, N 6.27; found C 82.25, H 4.50, N 6.28.

2,2′-Bis[4-(dimethylamino)phenyl]-7,7′-dinitro-9,9′-spirobifluorene (3): In a Schlenk tube, a stirred mixture of **8** (202 mg, 0.359 mmol), **10** (358 mg, 2.170 mmol), aqueous K_2CO_3 (1 M, 5 mL, 5 mmol), and $Pd(PPh_3)_4$ (23 mg, 0.020 mmol) in anhydrous THF (10 mL) was refluxed overnight under an inert atmosphere. After cooling to r.t., THF was removed under vacuum and the aqueous phase was extracted with CH_2Cl_2 (3 × 25 mL). The collected organic phases were dried with Na_2SO_4 and the solvent was removed under vacuum. The crude material was purified by chromatography (hexane/ethyl acetate, 5:1) to give **3** (167 mg, 67%) as an orange solid; m.p. 281–283 °C. ^{1}H NMR (400 MHz, $CDCl_3$, 25 °C): δ = 8.34 (dd, $J_{H,H}$ = 8.4, $J_{H,H}$ = 2.1 Hz, 2 H, 6-H, 6′-H), 7.98 (d, $J_{H,H}$ = 8.1 Hz, 2 H, 4-H, 4′-H), 7.97 (d, $J_{H,H}$ = 8.4 Hz, 2 H, 5-H, 5′-H), 7.70 (dd, $J_{H,H}$ = 8.1, $J_{H,H}$ = 1.6 Hz, 2 H, 3-H, 3′-H), 7.58 (d, $J_{H,H}$ = 2.1 Hz, 2 H, 8-H, 8′-H), 7.50 (d, $J_{H,H}$ = 8.9 Hz, 4 H, 2-H phenyl, 6-H phenyl), 6.96 (d, $J_{H,H}$ = 1.6 Hz, 2 H, 1-H, 1′-H), 6.58 (br. d, $J_{H,H}$ = 8.8 Hz, 4 H, 3-H phenyl, 5-H phenyl), 2.83 (s, 6 H, CH_3) ppm. ^{13}C NMR (101 MHz, $CDCl_3$, 25 °C): δ = 150.36 (q), 149.42 (q), 148.61 (q), 148.34 (q), 147.28 (q), 143.75 (q), 137.15 (q), 127.79 (2-C phenyl, 6-C phenyl), 127.72 (q), 127.01 (3-C, 3′-C), 124.71 (6-C, 6′-C), 122.09 (4-C, 4′-C), 121.81 (1-C, 1′-C), 120.22 (5-C, 5′-C), 119.61 (1-C, 1′-C), 112.55 (3-C phenyl, 5-C phenyl), 65.70 (9-C), 40.39 (CH_3) ppm. UV/Vis ($CHCl_3$): λ_{max} (ε, mol^{-1} dm^3 cm^{-1}) = 300 (40900), 410 (42600) nm. HRMS (ESI+): calcd. for $C_{41}H_{32}N_4O_4Na$ $[M + Na]^+$ 667.2316; found 667.2305. $C_{41}H_{32}N_4O_4$ (644.72): calcd. C 76.38, H 5.00, N 8.69; found C 76.55, H 5.09, N 8.71.

(*E*,*E*)-2,2′-Bis{2-[4-(dimethylamino)phenyl]ethen-1-yl}-7,7′-dinitro-9,9′-spirobifluorene (4): In a Schlenk tube, a mixture of **8** (249 mg, 0.442 mmol), K_2CO_3 (124 mg, 0.900 mmol), TBAB (285 mg, 0.885 mmol), anhydrous DMF (8 mL), and **11** (148 mg, 1.010 mmol) dissolved in anhydrous DMF (2 mL) was stirred at r.t. for 30 min. Then $Pd(OAc)_2$ (10 mg, 0.046 mmol) was added and the solution was vigorously stirred at 105 °C for 6 h. After cooling to r.t., DMF was removed under vacuum and the crude material was dissolved in CH_2Cl_2 (50 mL). After washed with water (2 × 20 mL), the organic phase was dried with Na_2SO_4 and the solvent was removed under vacuum. The crude material was purified by flash chromatography (hexane/ethyl acetate, 4:1) to give **4** (136 mg, 44%) as a dark solid; m.p. 234–239 °C. ^{1}H NMR (400 MHz, $CDCl_3$, 25 °C): δ = 8.33 (dd, $J_{H,H}$ = 8.4, $J_{H,H}$ = 2.1 Hz, 2 H, 6-H, 6′-H), 7.96 (d, $J_{H,H}$ = 8.4 Hz, 2 H, 5-H, 5′-H), 7.93 (d, $J_{H,H}$ = 8.1 Hz, 2 H, 4-H, 4′-H), 7.61 (dd, $J_{H,H}$ = 8.1, $J_{H,H}$ = 1.5 Hz, 2 H, 3-H, 3′-H), 7.57 (d, $J_{H,H}$ = 2.1 Hz, 2 H, 8-H, 8′-H), 7.29 (d, $J_{H,H}$ = 8.9 Hz, 4 H, 2-H phenyl, 6-H phenyl), 6.94 (d, $J_{H,H}$ = 16.2 Hz, 1 H, 1-H ethenyl), 6.90 (d, $J_{H,H}$ = 1.1 Hz, 2 H, 1-H, 1′-H), 6.77 (d, $J_{H,H}$ = 16.2 Hz, 1 H, 2-H ethenyl), 6.64 (br. d, $J_{H,H}$ = 8.9 Hz, 4 H, 3-H phenyl, 5-H phenyl), 2.95 (s, 6 H, CH_3) ppm. ^{13}C NMR (101 MHz, $CDCl_3$, 25 °C): δ = 150.29 (q), 149.25 (q), 148.55 (q), 148.16 (q), 147.28 (q), 140.88 (q), 137.75 (q), 130.66 (1-C ethenyl), 127.84 (2-C phenyl, 6-C phenyl), 127.10 (3-C, 3′-C), 125.09 (q), 124.76 (6-C, 6′-C), 123.19 (2-C ethenyl), 122.07 (4-C, 4′-C), 121.38 (1-C, 1′-C), 120.23 (5-C, 5′-C), 119.56 (8-C, 8′-C), 112.29 (3-C phenyl, 5-C phenyl), 65.43 (9-C), 40.35 (CH_3) ppm. UV/Vis ($CHCl_3$): λ_{max} (ε, mol^{-1} dm^3 cm^{-1}) = 325 (29200), 438 (43800) nm. HRMS (ESI+): calcd. for $C_{45}H_{37}N_4O_4$ $[M + H]^+$ 697.2809; found 697.2808; calcd. for $[M + H]^{2+}$ $C_{45}H_{38}N_4O_4$ 349.1441; found 349.1445. $C_{45}H_{36}N_4O_4$ (696.79): calcd. C 77.57, H 5.21, N 8.04; found C 77.55, H 5.22, N 8.06.

2,2′-Bis{2-[4-(dimethylamino)phenyl]ethyn-1-yl}-7,7′-dinitro-9,9′-spirobifluorene (5): In a Schlenk tube, a mixture of **8** (230 mg, 0.4085 mmol), $Pd(PPh_3)_2Cl_2$ (31 mg, 0.044 mmol), anhydrous DMF (20 mL), and NEt_3 (1 mL, 7.184 mmol) was stirred at r.t. for 5 min under an inert atmosphere. Compound **12** (241 mg, 1.657 mmol) was added and the solution was stirred at 90 °C for 5 h. After cooling to r.t., the solvent was removed under vacuum and the crude material was dissolved in CH_2Cl_2 and washed with water (3 × 25 mL). The organic phase was dried with Na_2SO_4 and the solvent was removed under vacuum. The crude material was purified by flash chromatography (CH_2Cl_2/hexane, 2:1) to afford **5** (130 mg, 46%) as an orange solid; m.p. >400 °C. ^{1}H NMR (400 MHz, $CDCl_3$, 25 °C): δ = 8.25 (dd, $J_{H,H}$ = 8.4, $J_{H,H}$ = 2.1 Hz, 2 H, 6-H, 6′-H), 7.92 (d, $J_{H,H}$ = 8.4 Hz, 2 H, 5-H, 5′-H), 7.91 (d, $J_{H,H}$ = 8.0 Hz, 2 H, 4-H, 4′-H), 7.57 (dd, $J_{H,H}$ = 8.0, $J_{H,H}$ = 1.4 Hz, 2 H, 3-H, 3′-H), 7.52 (d, $J_{H,H}$ = 2.1 Hz, 2 H, 8-H, 8′-H), 7.22 (d, $J_{H,H}$ = 9.0 Hz, 4 H, 2-H phenyl, 6-H phenyl), 6.95 (d, $J_{H,H}$ = 1.2 Hz, 2 H, 1-H, 1′-H), 6.54 (br. d, $J_{H,H}$ = 9.0 Hz, 4 H, 3-H phenyl, 5-H phenyl), 2.95 (s, 6 H, CH_3) ppm. ^{13}C NMR (101 MHz, $CDCl_3$, 25 °C): δ = 150.24 (q), 148.25 (q), 148.00 (q), 147.66 (q), 147.46 (q), 138.28 (q), 132.73 (2-C phenyl, 6-C phenyl), 132.10 (3-C, 3′-C), 126.84 (1-C, 1′-C), 126.20 (q), 124.81 (6-C, 6′-C), 121.65 (5-C, 5′-C), 120.63 (4-C, 4′-C), 119.52 (8-C, 8′-C), 111.61 (3-C phenyl, 5-C phenyl), 109.07 (q), 93.61 (2-C ethynyl), 87.24 (1-C ethynyl), 65.14 (9-C), 40.09 (CH_3) ppm. UV/Vis ($CHCl_3$): λ_{max} (ε, mol^{-1} dm^3 cm^{-1}) = 315 (52400), 415 (49600) nm. HRMS (ESI+): calcd. for $C_{45}H_{33}N_4O_4$ $[M + H]^+$ 693.2496; found 693.2485. $C_{45}H_{32}N_4O_4$ (692.76): calcd. C 78.02, H 4.66, N 8.09; found C 78.25, H 4.68, N 8.11.

9,9-Dimethyl-2-nitro-7-(piperidin-1-yl)fluorene (1a): In a Schlenk tube, a solution of $Pd_2(dba)_3$ (11 mg, 0.012 mmol) and P*t*Bu$_3$ (1 M in toluene, 19 μL, 0.019 mmol) in anhydrous toluene (2 mL) was stirred at r.t. for 20 min. The solution was transferred by using a cannula to a second Schlenk tube containing a mixture of **13** (196 mg, 0.535 mmol) and Cs_2CO_3 (328 mg, 1.006 mmol) and piperidine (65 μL, 0.657 mmol) in anhydrous toluene (5 mL). The solution was heated to reflux under vigorous stirring for 6 h. After cooling to r.t., saturated NH_4Cl (15 mL) was added and the mixture was extracted with ethyl acetate (3 × 15 mL). The collected organic phases were dried with Na_2SO_4 and the solvent was removed under vacuum. The crude material was purified by chromatography on silica (hexane/ethyl acetate, 96:4) to give **1a** (126 mg, 73%) as a red solid; m.p. 157–162 °C. ^{1}H NMR (400 MHz, $CDCl_3$, 25 °C): δ = 8.22–8.20 (m, 2 H, 1-H, 3-H), 7.65–7.61 (m, 2 H, 4-H, 5-H), 6.98 (d, $J_{H,H}$ = 2.3 Hz, 1 H, 8-H), 6.95 (dd, $J_{H,H}$ = 8.5, $J_{H,H}$ = 2.3 Hz, 1 H, 6-H), 3.31 (m, 4 H, piperidine), 1.76–1.72 (m, 4 H, piperidine), 1.68–1.64 (m, 2 H, piperidine), 1.50 (s, 6 H, CH_3) ppm. ^{13}C NMR (101 MHz, $CDCl_3$, 25 °C): δ = 157.00 (q), 153.86 (q), 153.48 (q), 146.53 (q), 145.72 (q), 127.47 (q), 123.69 (3-C), 122.32 (5-C), 118.45 (4-C), 118.06 (1-C), 115.25 (6-C), 109.65 (8-C), 50.19 (2-C piperidine, 6-C piperidine), 47.11 (9-C), 27.04 (CH_3), 25.75 (3-C piperidine, 5-C piperidine), 24.31 (4-C piperi-

 © 2010 Wiley-VCH Verlag GmbH & Co. KGaA, Weinheim

dine) ppm. UV/Vis ($CHCl_3$): λ_{max} (ε, $mol^{-1}\,dm^3\,cm^{-1}$) = 272 (16100), 418 (25800) nm. HRMS (ESI+): calcd. for $[M + H]^+$ $C_{20}H_{23}N_2O_2$ 323.1754; found 323.1755. $C_{20}H_{22}N_2O_2$ (322.40): calcd. C 74.51, H 6.88, N 8.69; found C 74.55, H 6.89, N 8.71.

7-[4-(Diphenylamino)phenyl]-9,9-dimethyl-2-nitrofluorene (2a): In a Schlenk tube, a stirred mixture of **13** (158 mg, 0.434 mmol), **9** (254 mg, 0.878 mmol), aqueous K_2CO_3 (1 M, 2.6 mL, 2.6 mmol), and $Pd(PPh_3)_4$ (22 mg, 0.019 mmol) in anhydrous THF (5 mL) was refluxed for 5 h under an inert atmosphere. After cooling to r.t., THF was removed under vacuum and the aqueous phase was extracted with CH_2Cl_2 (2 × 10 mL). The collected organic phases were dried with Na_2SO_4 and the solvent was removed under vacuum. The crude material was purified by chromatography (hexane/ethyl acetate, 95:5) to afford **2a** (145 mg, 69%) as an orange solid; m.p. 224–228 °C. ^1H NMR (400 MHz, $CDCl_3$, 25 °C): δ = 8.31 (d, $J_{H,H}$ = 2.0 Hz, 1 H, 1-H), 8.28 (dd, $J_{H,H}$ = 8.3, $J_{H,H}$ = 2.1 Hz, 1 H, 3-H), 7.84 (d, $J_{H,H}$ = 7.9 Hz, 1 H, 5-H), 7.82 (d, $J_{H,H}$ = 8.3 Hz, 1 H, 4-H), 7.69 (d, $J_{H,H}$ = 1.5 Hz, 1 H, 8-H), 7.63 (dd, $J_{H,H}$ = 7.9, $J_{H,H}$ = 1.6 Hz, 1 H, 6-H), 7.55 (d, $J_{H,H}$ = 8.7 Hz, 2 H, PhH), 7.32–7.28 (m, 4 H), 7.20–7.16 (m, 6 H), 7.07 (br. t, $J_{H,H}$ = 7.3 Hz, 2 H), 1.59 (s, 6 H, fluorene-CH_3) ppm. ^{13}C NMR (101 MHz, $CDCl_3$, 25 °C): δ = 155.84 (q), 154.78 (q), 147.71 (q), 147.57 (q), 147.06 (q), 145.62 (q), 142.18 (q), 135.53 (q), 134.57 (q), 129.38 (Ph), 127.96 (Ph), 126.32 (6-C), 124.62 (Ph), 123.70 (Ph), 123.55 (3-C), 123.21 (Ph), 121.80 (5-C), 121.13 (8-C), 120.01 (4-C), 118.33 (1-C), 47.42 (9-C), 26.91 (CH_3) ppm. UV/Vis ($CHCl_3$): λ_{max} (ε, $mol^{-1}\,dm^3\,cm^{-1}$) = 311 (31700), 403 (25800) nm. HRMS (ESI+): calcd. for $[M + H]^+$ $C_{33}H_{27}N_2O_2$ 483.2067; found 483.2053. $C_{33}H_{27}N_2O_2$ (483.58): calcd. C 82.13, H 5.43, N 5.81; found C 82.00, H 5.44, N 5.80.

2-[4-(Dimethylamino)phenyl]-9,9-dimethyl-7-nitrofluorene (3a): In a Schlenk tube, a stirred mixture of **13** (201 mg, 0.552 mmol), **10** (272 mg, 1.650 mmol), aqueous K_2CO_3 (1 M, 3.3 mL, 3.3 mmol), and $Pd(PPh_3)_4$ (25 mg, 0.022 mmol) in anhydrous THF (6 mL) was refluxed overnight under an inert atmosphere. After cooling to r.t., THF was removed under vacuum and the aqueous phase was extracted with CH_2Cl_2 (2 × 10 mL). The collected organic phases were dried with Na_2SO_4 and the solvent was removed under vacuum. The crude material was purified by chromatography (hexane/ethyl acetate, 95:5) to give **3a** (126 mg, 64%) as an orange solid; m.p. 215–221 °C. ^1H NMR (400 MHz, $CDCl_3$, 25 °C): δ = 8.30 (d, $J_{H,H}$ = 2.0 Hz, 1 H, 8-H), 8.27 (dd, $J_{H,H}$ = 8.3, $J_{H,H}$ = 2.1 Hz, 1 H, 6-H), 7.80 (m, 2 H, 4-H fluorene, 5-H fluorene), 7.66 (d, $J_{H,H}$ = 1.5 Hz, 1 H, 1-H), 7.63–7.58 (m, 3 H, 3-H, 2-H phenyl, 6-H phenyl), 6.85 (br. d, $J_{H,H}$ = 8.1 Hz, 2 H, 2-H phenyl, 6-H phenyl), 3.04 (s, 6 H, N-CH_3), 1.59 (s, 6 H, fluorene-CH_3) ppm. ^{13}C NMR (101 MHz, $CDCl_3$, 25 °C): δ = 155.83 (q), 154.70 (q), 146.87 (q), 145.87 (q), 142.78 (q), 134.74 (q), 127.92 (2-C phenyl, 6-C phenyl), 125.87 (3-C), 123.52 (6-C), 121.72 (5-C), 120.62 (1-C), 119.78 (4-C), 118.28 (8-C), 112.79 (3-C phenyl, 5-C phenyl), 47.34 (9-C), 40.57 (CH_3-N), 26.92 (CH_3-fluorene) ppm. UV/Vis ($CHCl_3$): λ_{max} (ε, $mol^{-1}\,dm^3\,cm^{-1}$) = 297 (23300), 402 (26100) nm. HRMS (ESI+): calcd. for $[M + H]^+$ $C_{23}H_{23}N_2O_2$ 359.1754; found 359.1754. $C_{23}H_{22}N_2O_2$ (358.43): calcd. C 77.07, H 6.19, N 7.82; found C 77.00, H 6.20, N 7.84.

(*E*)-2-{2-[4-(Dimethylamino)phenyl]ethen-1-yl}-9,9-dimethyl-7-nitrofluorene (4a): In a Schlenk tube, a mixture of **13** (162 mg, 0.443 mmol), K_2CO_3 (65 mg, 0.472 mmol), TBAB (144 mg, 0.447 mmol), anhydrous DMF (5 mL), and **11** (73 mg, 0.496 mmol) dissolved in anhydrous DMF (2 mL) was stirred at r.t. for 30 min. Then $Pd(OAc)_2$ (5 mg, 0.024 mmol) was added and the solution was vigorously stirred at 105 °C for 6 h. After cooling to r.t., DMF was removed under vacuum and the crude material was dissolved in CH_2Cl_2 (50 mL), washed with water (2 × 20 mL), and the organic phase was dried with Na_2SO_4 and the solvent removed under vacuum. The crude material was purified by chromatography on silica (hexane/ethyl acetate, 9:1) to give **4a** (80 mg, 47%) as an orange solid; m.p. 212–219 °C. ^1H NMR (400 MHz, $CDCl_3$, 25 °C): δ = 8.29 (d, $J_{H,H}$ = 2.0 Hz, 1 H, 8-H), 8.26 (dd, $J_{H,H}$ = 8.3, $J_{H,H}$ = 2.1 Hz, 1 H, 6-H), 7.75 (br. t, $J_{H,H}$ = 8.1 Hz, 2 H, 4-H, 5-H), 7.59 (d, $J_{H,H}$ = 1.1 Hz, 1 H, 1-H), 7.52 (dd, $J_{H,H}$ = 8.0, $J_{H,H}$ = 1.5 Hz, 1 H, 3-H), 7.46 (d, $J_{H,H}$ = 8.8 Hz, 2 H, 2-H phenyl, 6-H phenyl), 7.17 (d, $J_{H,H}$ = 16.2 Hz, 1 H, 1-H ethenyl), 7.01 (d, $J_{H,H}$ = 16.2 Hz, 1 H, 2-H ethenyl), 6.74 (d, $J_{H,H}$ = 8.8 Hz, 2 H, 3-H phenyl, 5-H phenyl), 3.02 (s, 6 H, N-CH_3), 1.58 (s, 6 H, fluorene-CH_3) ppm. ^{13}C NMR (101 MHz, $CDCl_3$, 25 °C): δ = 155.72 (q), 154.72 (q), 150.36 (q), 146.84 (q), 145.78 (q), 139.83 (q), 135.41 (q), 129.98 (1-C ethenyl), 127.82 (2-C phenyl, 6-C phenyl), 125.87 (3-C), 125.40 (q), 123.99 (2-C ethenyl), 123.53 (6-C), 121.68 (4-C), 120.09 (1-C), 119.76 (5-C), 118.27 (8-C), 112.41 (3-C phenyl, 5-C phenyl), 47.22 (9-C), 40.42 (CH_3-N), 26.89 (CH_3-fluorene) ppm. UV/Vis ($CHCl_3$): λ_{max} (ε, $mol^{-1}\,dm^3\,cm^{-1}$) = 325 (18300), 429 (27900) nm. HRMS (ESI+): calcd. for $[M + H]^+$ $C_{25}H_{25}N_2O_2$ 385.1910; found 385.1902. $C_{25}H_{24}N_2O_2$ (384.47): calcd. C 78.10, H 6.29, N 7.29; found C 78.30, H 6.30, N 7.31.

2-{2-[4-(Dimethylamino)phenyl]ethyn-1-yl}-9,9-dimethyl-7-nitrofluorene (5a): In a Schlenk tube, a mixture of **13** (151 mg, 0.415 mmol), $Pd(PPh_3)_2Cl_2$ (15 mg, 0.022 mmol), anhydrous DMF (15 mL), and NEt_3 (0.59 mL, 4.24 mmol) was stirred at r.t. for 5 min under an inert atmosphere. Compound **12** (123 mg, 0.846 mmol) was added and the solution was stirred at 90 °C for 6 h. After cooling to r.t., the solvent was removed under vacuum and the crude material was dissolved in ethyl acetate (50 mL) and washed with water (3 × 20 mL). The organic phase was dried with Na_2SO_4 and the solvent was removed under vacuum. The crude material was purified by flash chromatography (hexane/CH_2Cl_2, 9:1) to give **5a** (86 mg, 54%) as an orange solid; m.p. 236–239 °C. ^1H NMR (400 MHz, $CDCl_3$, 25 °C): δ = 8.29 (d, $J_{H,H}$ = 2.0 Hz, 1 H, 8-H), 8.26 (dd, $J_{H,H}$ = 8.3, $J_{H,H}$ = 2.1 Hz, 1 H, 6-H), 7.78 (d, $J_{H,H}$ = 8.3 Hz, 1 H, 5-H), 7.75 (d, $J_{H,H}$ = 7.9 Hz, 1 H, 4-H), 7.62 (d, $J_{H,H}$ = 0.9 Hz, 1 H, 1-H), 7.54 (dd, $J_{H,H}$ = 7.9, $J_{H,H}$ = 1.4 Hz, 1 H, 3-H), 7.44 (d, $J_{H,H}$ = 8.9 Hz, 2 H, 2-H phenyl, 6-H phenyl), 6.68 (d, $J_{H,H}$ = 8.9 Hz, 2 H, 3-H phenyl, 5-H phenyl), 3.02 (s, 6 H, N-CH_3), 1.56 (s, 6 H, fluorene-CH_3) ppm. ^{13}C NMR (101 MHz, $CDCl_3$, 25 °C): δ = 155.07 (q), 154.82 (q), 150.29 (q), 147.17 (q), 145.28 (q), 135.98 (q), 132.85 (2-C phenyl, 6-C phenyl), 130.84 (3-C), 125.78 (1-C), 125.24 (q), 123.51 (6-C), 121.33 (4-C), 120.19 (5-C), 118.32 (8-C), 111.85 (3-C phenyl, 5-C phenyl), 109.65 (q), 92.55 (2-C ethynyl), 87.82 (1-C ethynyl), 47.33 (9-C), 40.19 (CH_3-N), 26.73 (CH_3-fluorene) ppm. UV/Vis ($CHCl_3$): λ_{max} (ε, $mol^{-1}\,dm^3\,cm^{-1}$) = 311 (26400), 405 (27700) nm. HRMS (ESI^+): calcd. for $[M + H]^+$ $C_{25}H_{23}N_2O_2$ 383.1754; found 323.1746. $C_{25}H_{22}N_2O_2$ (382.45): calcd. C 78.51, H 5.80, N 7.32; found C 78.70, H 5.80, N 7.34.

Acknowledgments

Financial support by Fondazione CARIPLO (project title: "Preparazione strutture altamente organizzate – PRESTO") and Fondo per gli Investimenti della Ricerca di Base (FIRB), project number RBIP0642YL (title: "Sorgenti di luce innovative ad alta efficienza per dispositivi illuminanti a stato solido con impiego civile ed automotive – LUCI" and "Sviluppo di componenti e soluzioni tecnologiche integrate per display di nuova generazione – NODIS") of Ministero dell'Università e della Ricerca (MIUR) is gratefully acknowledged.

 © 2010 Wiley-VCH Verlag GmbH & Co. KGaA, Weinheim

[1] J. Zyss, P. Kelley, P. F. Liao, *Molecular Nonlinear Optics: Materials, Physics and Devices*, Academic Press, **1993**.

[2] S. R. Marder, B. Kippelen, A. K. Y. Jen, N. Peyghambarian, *Nature* **1997**, *388*, 845–851.

[3] O. Mongin, L. Porres, M. Charlot, C. Katan, M. Blanchard-Desce, *Chem. Eur. J.* **2007**, *13*, 1481–1498.

[4] F. Tessore, D. Roberto, R. Ugo, M. Pizzotti, S. Quici, M. Cavazzini, S. Bruni, F. De Angelis, *Inorg. Chem.* **2005**, *44*, 8967–8978.

[5] A. Facchetti, L. Beverina, M. E. van der Boom, P. Dutta, G. Evmenenko, A. D. Shukla, C. E. Stern, G. A. Pagani, T. J. Marks, *J. Am. Chem. Soc.* **2006**, *128*, 2142–2153.

[6] J. A. Davies, A. Elangovan, P. A. Sullivan, B. C. Olbricht, D. H. Bale, T. R. Ewy, C. M. Isborn, B. E. Eichinger, B. H. Robinson, P. J. Reid, X. Li, L. R. Dalton, *J. Am. Chem. Soc.* **2008**, *130*, 10565–10575.

[7] J. L. Oudar, D. S. Chemla, *J. Chem. Phys.* **1977**, *66*, 2664–2668.

[8] P. J. A. Kenis, E. G. Kerver, B. H. M. Snellink-RuÎl, G. J. v. Hummel, S. Harkema, M. C. Flipse, R. H. Woudenberg, J. F. J. Engbersen, D. N. Reinhoudt, *Eur. J. Org. Chem.* **1998**, 1089–1098.

[9] G. Hennrich, M. T. Murillo, P. Prados, H. Al-Saraierh, A. El-Dali, D. W. Thompson, J. Collins, P. E. Georghiou, A. Teshome, I. Asselberghs, K. Clays, *Chem. Eur. J.* **2007**, *13*, 7753–7761.

[10] J. O. Morley, M. Naji, *J. Phys. Chem. A* **1997**, *101*, 2681–2685.

[11] M. Ronchi, M. Pizzotti, A. O. Biroli, S. Righetto, R. Ugo, P. Mussini, M. Cavazzini, E. Lucenti, M. Salsa, P. Fantucci, *J. Phys. Chem. C* **2009**, *113*, 2745–2760.

[12] T. Morotti, V. Calabrese, M. Cavazzini, D. Pedron, M. Cozzuol, A. Licciardello, N. Tuccitto, S. Quici, *Dalton Trans.* **2008**, 2974–2982.

[13] H. E. Katz, M. L. Schilling, *Chem. Mater.* **1993**, *5*, 1162–1166.

[14] H. E. Katz, *Chem. Mater.* **1994**, *6*, 2227–2232.

[15] P. W. Zhu, M. E. van der Boom, H. Kang, G. Evmenenko, P. Dutta, T. J. Marks, *Chem. Mater.* **2002**, *14*, 4982–4989.

[16] M. Halter, Y. Liao, R. M. Plocinik, D. C. Coffey, S. Bhattacharjee, U. Mazur, G. J. Simpson, B. H. Robinson, S. L. Keller, *Chem. Mater.* **2008**, *20*, 1778–1787.

[17] T. P. I. Saragi, T. Spehr, A. Siebert, T. Fuhrmann-Lieker, J. Salbeck, *Chem. Rev.* **2007**, *107*, 1011–1065.

[18] C.-L. Chiang, S.-M. Tseng, C.-T. Chen, C.-P. Hsu, C.-F. Shu, *Adv. Funct. Mater.* **2008**, *18*, 248–257.

[19] R. Pudzich, J. Salbeck, *Synth. Met.* **2003**, *138*, 21–31.

[20] C.-L. Chiang, M.-F. Wu, D.-C. Dai, Y.-S. Wen, J.-K. Wang, C.-T. Chen, *Adv. Funct. Mater.* **2005**, *15*, 231–238.

[21] Y.-T. Lee, C.-L. Chiang, C.-T. Chen, *Chem. Commun.* **2008**, 217–219.

[22] Y. L. Liao, C. Y. Lin, K. T. Wong, T. H. Hou, W. Y. Hung, *Org. Lett.* **2007**, *9*, 4511–4514.

[23] L. Otero, L. Sereno, F. Fungo, Y. L. Liao, C. Y. Lin, K. T. Wong, *Chem. Mater.* **2006**, *18*, 3495–3502.

[24] J. Abe, Y. Shirai, N. Nemoto, Y. Nagase, *J. Phys. Chem. A* **1997**, *101*, 1–4.

[25] J. K. Feng, X. Y. Sun, A. H. Ren, K. Q. Yu, C. C. Sun, *J. Mol. Struct.* **1999**, *489*, 247–254.

[26] S. Y. Kim, M. Lee, B. H. Boo, *J. Chem. Phys.* **1998**, *109*, 2593–2595.

[27] Y. Luo, P. Norman, H. Agren, *Chem. Phys. Lett.* **1999**, *303*, 616–620.

[28] W. Fu, J. K. Feng, G. B. Pan, *J. Mol. Struct.* **2001**, *545*, 157–165.

[29] J. Pei, J. Ni, X. H. Zhou, X. Y. Cao, Y. H. Lai, *J. Org. Chem.* **2002**, *67*, 8104–8113.

[30] C. L. Chiang, C. F. Shu, C. T. Chen, *Org. Lett.* **2005**, *7*, 3717–3720.

[31] F. K. Sutcliffe, H. M. Shahidi, D. Patterson, *J. Soc. Dyers Colour.* **1978**, *94*, 306–309.

[32] A. L. Reiff, E. M. Garcia-Frutos, J. M. Gil, O. P. Anderson, L. S. Hegedus, *Inorg. Chem.* **2005**, *44*, 9162–9174.

[33] Y. Kim, S. Park, Y. Han, Y. Do, *Bull. Korean Chem. Soc.* **2004**, *25*, 1648–1652.

[34] F. Thiemann, T. Piehler, D. Haase, W. Saak, A. Lutzen, *Eur. J. Org. Chem.* **2005**, 1991–2001.

[35] G. Hallas, J. D. Hepworth, D. R. Waring, *J. Chem. Soc. B* **1970**, 975–979.

[36] V. C. Marhevka, N. A. Ebner, R. D. Sehon, P. E. Hanna, *J. Med. Chem.* **1985**, *28*, 18–24.

[37] B. J. Lynch, P. L. Fast, M. Harris, D. G. Truhlar, *J. Phys. Chem. A* **2000**, *104*, 4811–4815.

[38] M. Cossi, N. Rega, G. Scalmani, V. Barone, *J. Comput. Chem.* **2003**, *24*, 669–681.

[39] G. Park, C. S. Ra, B. R. Cho, *Bull. Korean Chem. Soc.* **2003**, *24*, 1671–1674.

[40] R. Hoffmann, A. Imamura, G. D. Zeiss, *J. Am. Chem. Soc.* **1967**, *89*, 5215–5220.

[41] H. E. Simmons, T. Fukunaga, *J. Am. Chem. Soc.* **1967**, *89*, 5208–5215.

[42] K. D. Singer, A. F. Garito, *J. Chem. Phys.* **1981**, *75*, 3572–3580.

[43] B. F. Levine, C. G. Bethea, *Appl. Phys. Lett.* **1974**, *24*, 445–447.

[44] I. Ledoux, J. Zyss, *Chem. Phys.* **1982**, *73*, 203–213.

[45] C. M. Whitaker, E. V. Patterson, K. L. Kott, R. J. McMahon, *J. Am. Chem. Soc.* **1996**, *118*, 9966–9973.

[46] P. N. Prasad, *Introduction to Nonlinear Optical Effects in Molecules and Polymers*, Wiley, New York, N. Y., **1990**.

[47] E. A. Guggenheim, *Trans. Faraday Soc.* **1949**, *45*, 714–720.

[48] H. B. Thompson, *J. Chem. Educ.* **1966**, *43*, 66–73.

[49] A. Willetts, J. E. Rice, D. M. Burland, D. P. Shelton, *J. Chem. Phys.* **1992**, *97*, 7590–7599.

[50] R. Ditchfield, W. J. Hehre, J. A. Pople, *J. Chem. Phys.* **1971**, *54*, 724–728.

[51] A. D. Becke, *J. Chem. Phys.* **1993**, *98*, 5648–5652.

[52] M. J. Frisch, G. W. Trucks, H. B. Schlegel, G. E. Scuseria, M. A. Robb, J. R. Cheeseman, J. A. Montgomery Jr., T. Vreven, K. N. Kudin, J. C. Burant, J. M. Millam, S. S. Iyengar, J. Tomasi, V. Barone, B. Mennucci, M. Cossi, G. Scalmani, N. Rega, G. A. Petersson, H. Nakatsuji, M. Hada, M. Ehara, K. Toyota, R. Fukuda, J. Hasegawa, M. Ishida, T. Nakajima, Y. Honda, O. Kitao, H. Nakai, M. Klene, X. Li, J. E. Knox, H. P. Hratchian, J. B. Cross, C. Adamo, J. Jaramillo, R. Gomperts, R. E. Stratmann, O. Yazyev, A. J. Austin, R. Cammi, C. Pomelli, J. W. Ochterski, P. Y. Ayala, K. Morokuma, G. A. Voth, P. Salvador, J. J. Dannenberg, V. G. Zakrzewski, S. Dapprich, A. D. Daniels, M. C. Strain, O. Farkas, D. K. Malick, A. D. Rabuck, K. Raghavachari, J. B. Foresman, J. V. Ortiz, Q. Cui, A. G. Baboul, S. Clifford, J. Cioslowski, B. B. Stefanov, G. Liu, A. Liashenko, P. Piskorz, I. Komaromi, R. L. Martin, D. J. Fox, T. Keith, M. A. Al-Laham, C. Y. Peng, A. Nanayakkara, M. Challacombe, P. M. W. Gill, B. Johnson, W. Chen, M. W. Wong, C. Gonzalez, J. A. Pople, *Gaussian 03*, Gaussian, Inc., Pittsburgh, **2003**.

[53] M. Pastore, E. Mosconi, F. De Angelis, M. Gräetzel, *J. Phys. Chem. C* **2010**, *114*, 7205–7212.

Received: March 10, 2010
Published Online: June 11, 2010

 © 2010 Wiley-VCH Verlag GmbH & Co. KGaA, Weinheim